This article is published as part of the *Dalton Transactions* themed issue entitled:

Self-Assembly in Inorganic Chemistry

Guest Editors Paul Kruger and Thorri Gunnlaugsson

Published in issue 45, 2011 of *Dalton Transactions*

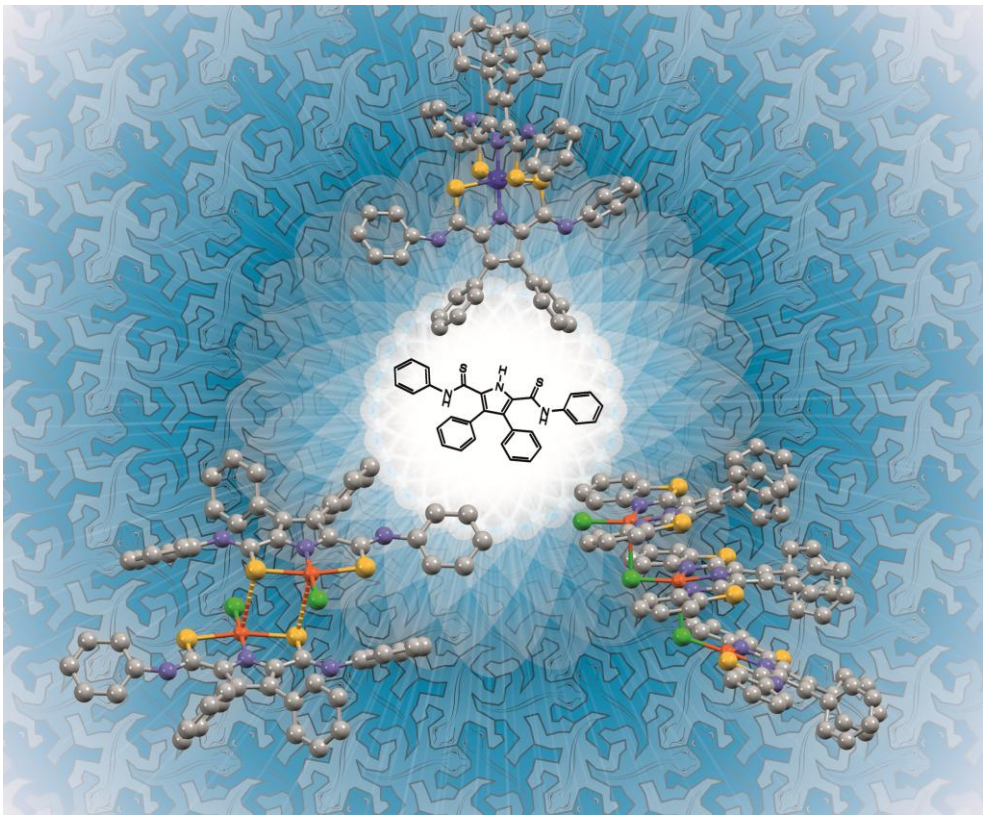

Image reproduced with permission of Mark Ogden

Articles in the issue include:

PERSPECTIVE:

ARTICLES:

Visit the *Dalton Transactions* website for more cutting-edge inorganic and organometallic research
www.rsc.org/dalton

Dalton Transactions

Dynamic Article Links

Cite this: *Dalton Trans.*, 2011, **40**, 12028

www.rsc.org/dalton

COMMUNICATION

Control of the transition temperatures of metallomesogens by specific interface design: application to Mn_{12} single molecule magnets†

E. Terazzi,*[a] T. B. Jensen,[a] B. Donnio,[b] K. Buchwalder,[a] C. Bourgogne,[b] G. Rogez,[b] B. Heinrich,[b] J. Gallani[b] and C. Piguet[a]

Received 13th May 2011, Accepted 21st June 2011
DOI: 10.1039/c1dt10908a

Reaction of the Single Molecule Magnet $[Mn_{12}O_{12}(CH_3CO_2)_{16}(H_2O)_4]$ (Mn_{12}) with mesogenic dendritic ligands L*i* **(*i* = 4, 5) quantitatively yields functional clusters $[Mn_{12}O_{12}(Li\text{-}H)_{16}(H_2O)_4]$ (*i* = 4, 5) that self-organize into a thermotropic SmA-type liquid crystalline phase. The perturbation of the molecular interface by methylation of the terminal mesogenic cyanobiphenyl groups induces a significant decrease of the clearing temperature without affecting the magnetic properties and the supramolecular organization of the Mn_{12}-based clusters.**

The combination of metal ions with organic ligands using coordination chemistry yields discrete and sophisticated complexes with original magnetic or optical properties. With some additional tailoring, weak intermolecular forces can be controlled and the material driven to self-assemble into large supramolecular architectures. Mastering these two areas has become essential in the development of new functional hybrid materials[1] and directed self-organization by encapsulation with amphiphilic molecules is currently exploited for introducing functional inorganic devices into novel liquid crystalline phases[2,3,4] adapted for practical applications like molecular electronics.[5] An important challenge in this domain concerns the self-organization of Single Molecule Magnets (SMMs) for high density information storage.[6] These compounds are able to retain a stable magnetization below a characteristic temperature, known as the blocking temperature,[7] and can be envisioned as the ultimate qbits. However, SMMs have to be first deposited onto surfaces as self-organized monolayers, a process which may take place only when some fluidity exists in the sample.[8] Liquid crystals are known to possess both fluidity and organization and can consequently be helpful in this context. The appearance of a liquid crystalline state is usually related to the presence of at least two antagonist parts in the same compound, like one or several flexible aliphatic chains connected to a highly polarisable but rather rigid polyaromatic scaffold. According to a rough thermodynamic approach,[9] the melting point ($T_m = \Delta H_m/\Delta S_m$) results from the decorrelation between the aliphatic chains while the clearing point ($T_c = \Delta H_c/\Delta S_c$) reflects the decorrelation between the residual aromatic interactions. Following this concept, and inspired by the pioneering work of Saez and Goodby[10] and Chuard *et al.*[11] concerning liquid crystalline octasilesquioxanes and C_{60} fullerenes respectively, some of us recently succeeded in preparing a liquid crystalline derivative of the original $[Mn_{12}O_{12}(CH_3CO_2)_{16}(H_2O)_4]$ cluster,[12] in which the sixteen axial and equatorial acetates were replaced with the mesogenic ligand **L1** to give $[Mn_{12}O_{12}(\mathbf{L1}\text{-H})_{16}(H_2O)_4]$. The compound retained the SMM's magnetic properties (Scheme 1) and displayed a supramolecular lamellar-like organization.[13] Subsequent attempts to transpose bulk ordering onto surfaces were limited by the impossibility of reaching the clearing point without decomposing the clusters.[14] In their quest to design lanthanide-containing metallomesogens with nematic (N) liquid crystalline order, Piguet *et al.* synthesized dendritic ligands **L*i*** (*i* = 2, 3)

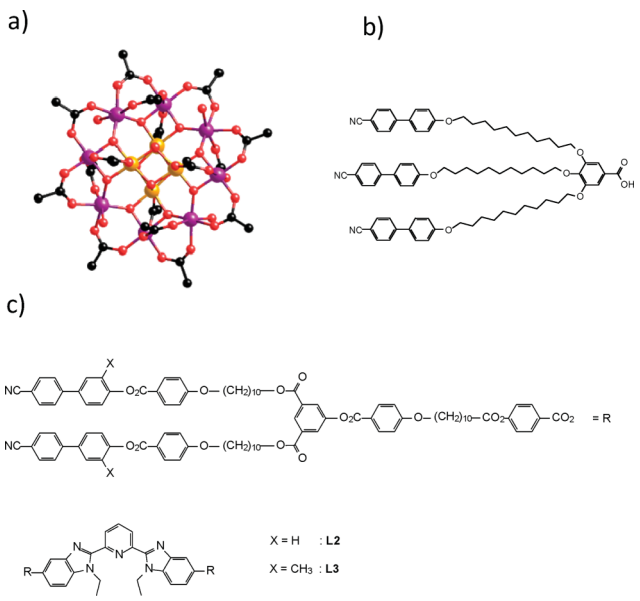

Scheme 1 (a) Structure of the $[Mn_{12}O_{12}(CH_3CO_2)_{16}(H_2O)_4]$ cluster.[8] (b) Structure of ligand **L1** (c) Structures of dendritic ligands **L2** and **L3**.

[a]*Department of Inorganic, Analytical and Applied Chemistry, University of Geneva, 30 quai E. Ansermet, CH-1211 Geneva 4, (Switzerland). E-mail: Emmanuel.Terazzi@unige.ch*
[b]*Institut de Physique et Chimie des Matériaux de Strasbourg (IPCMS), UMR 7504 (CNRS-Université de Strasbourg), 23 rue du Loess, BP43, 67034, Strasbourg cedex 2, France*

† Electronic supplementary information (ESI) available: Experimental procedures and characterization processes (EA, NMR, TGA, POM, SA-XRD, SQUID, DSC) for **L*i*** and $[Mn_{12}O_{12}(\mathbf{Li}\text{-H})_{16}(H_2O)_4]$ (*i* = 4, 5) (Tables S1–S22, Figs S1–S10). See DOI: 10.1039/c1dt10908a

with the idea that the perturbation of the interface induced by the methylation of classical cyanobiphenyl mesogens may affect the phase sequence and significantly decrease the clearing temperatures (Scheme 1c).[15] And indeed, not only was a nematic phase induced in some lanthanidomesogens, but thermal stability was also considerably enhanced.

In order to exploit this strategy for producing fluid mesophases of Mn_{12} clusters at low temperature, structurally related ligands **L*i*** (i = 4, 5, Scheme 2) were synthesized[15] and the associated dodecanuclear clusters $[Mn_{12}O_{12}(\mathbf{L}i\text{-H})_{16}(H_2O)_4]$ (i = 4, 5) were obtained by ligand exchange in a CH_2Cl_2–toluene solvent mixture, with a large excess of **L*i*** (i = 4, 5). Elemental analyses for the two new clusters agree with the expected $[Mn_{12}O_{12}(\mathbf{L}i\text{-H})_{16}(H_2O)_4]\cdot xH_2O$ (i = 4, 5) stoichiometries, thus confirming that all acetate anions have been replaced with the new lipophilic carboxylate ligands (Table S1, ESI†).

Due to the presence of the slow-relaxing paramagnetic manganese ions, the ^{1}H NMR signals of the protons located close to the paramagnetic cluster are too broad to be observed, but the major part of the peripheral protons attached to the remote semi-dendrimeric moieties in $[\mathbf{L}i\text{-H}]^-$ (i = 4, 5) can be detected for $[Mn_{12}O_{12}(\mathbf{L}i\text{-H})_{16}(H_2O)_4]$ (i = 4, 5) in chloroform solution (Fig. S1, ESI†). Interestingly, the ^{1}H NMR signal of the methylene groups connected to the anionic terephthalic binding unit disappears in the clusters, which is diagnostic for its coordination to the paramagnetic centres (Fig. S1, ESI†). Moreover, the magnetic characterization of $[Mn_{12}O_{12}(\mathbf{L5}\text{-H})_{16}(H_2O)_4]$ confirms that the overall Mn_{12} structure and SMM behaviour are preserved. In the 2–8 K temperature range, an out-of-phase ac susceptibility signal (χ'') was detected in the 1 to 1000 Hz frequency domain (Fig. S2, ESI†). This signal is characteristic of the slowing down of the relaxation of the magnetization and is considered as the signature of SMM behaviour.[7,16] The magnetization relaxation time τ follows the Arrhenius law, $\tau = \tau_0 \exp(-(U_{eff}/kT)$ (Fig. S2, ESI†). The fit of the ac susceptibility data provides an effective anisotropy barrier U_{eff} = 56 K, which is standard for Mn_{12} clusters (Fig S3, ESI,† k is Boltzmann's constant, $\tau_0 = 6.7 \times 10^{-9}$ s is the pre-exponential factor). The $\chi_{ac}T$ value remains constant at all frequencies above 8 K ($\chi_{ac} = \sqrt{(\chi')^2 + (\chi'')^2}$, Fig. S4, ESI†), a domain of temperature for which the ground state is assumed to be the only thermally populated level. Consequently $\chi'T$ = 38 emu K mol^{-1} can be used for calculating S_{tot} = 9 and g = 1.83 for $[Mn_{12}O_{12}(\mathbf{L5}\text{-H})_{16}(H_2O)_4]$ in complete agreement with closely related Mn_{12} clusters.[13,17] Finally, the magnetization curve recorded at 1.8 K shows a hysteresis loop with a coercive field of 0.13 Tesla, which is characteristic of a randomly oriented polycrystalline Mn_{12} sample (Fig. S5, ESI†).[13,16,17]

ThermoGravimetric Analyses (TGA) indicate that the clusters $[Mn_{12}O_{12}(\mathbf{L}i\text{-H})_{16}(H_2O)_4]$ are stable at temperatures below 250 °C (Fig. S6, ESI†), while Differential Scanning Calorimetry (DSC, Fig. 1) combined with Polarized Optical Microscopy (POM) confirms the formation of fluid birefringent and homogeneous textures (Fig. S7, ESI†) in the 40–200 °C range for i = 4, and in the 35–140 °C range for i = 5, which are compatible with the

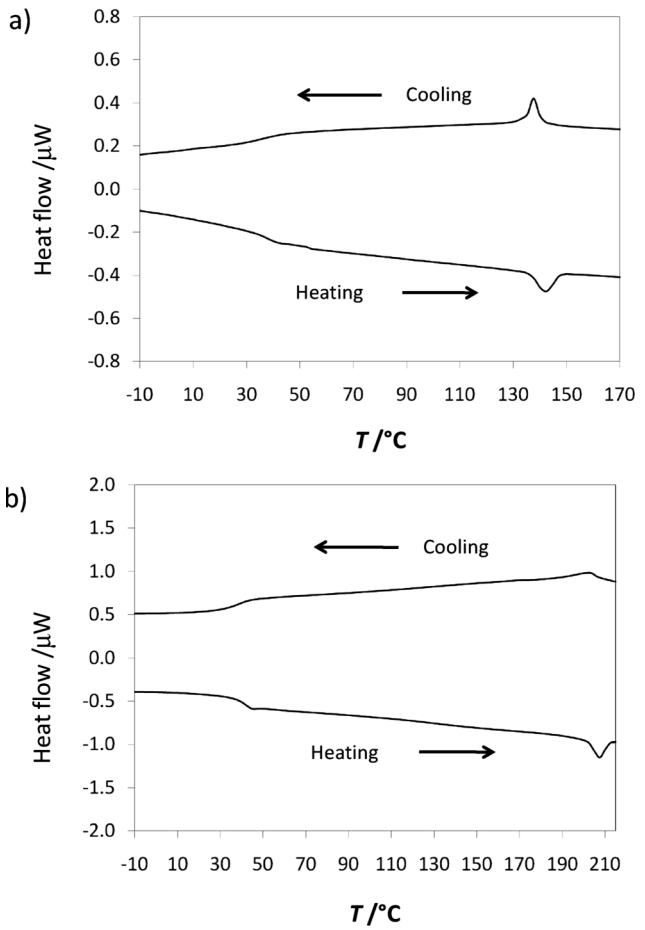

Fig. 1 (a) DSC trace of $[Mn_{12}O_{12}(\mathbf{L5}\text{-H})_{16}(H_2O)_4]$ (5 °C min^{-1} under N_2) (b) DSC trace of $[Mn_{12}O_{12}(\mathbf{L4}\text{-H})_{16}(H_2O)_4]$ (5 °C min^{-1} under N_2).

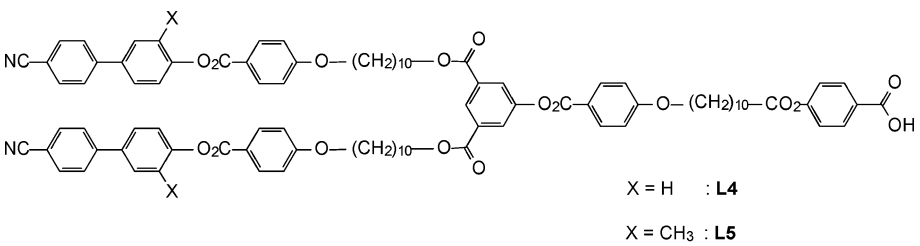

$$[Mn_{12}O_{12}(CH_3CO_2)_{16}(H_2O)_4] + 16\ Li \rightleftharpoons [Mn_{12}O_{12}(Li\text{-H})_{16}(H_2O)_4] + 16\ CH_3CO_2H$$

Scheme 2 Ligand exchange reaction producing $[Mn_{12}O_{12}(\mathbf{L}i\text{-H})_{16}(H_2O)_4]$ (i = 4, 5).

Table 1 Temperatures, enthalpy and entropy changes of the phase transitions observed for the ligands **L*i*** (i = 4, 5) and their clusters $[Mn_{12}O_{12}(\mathbf{L}i\text{-H})_{16}(H_2O)_4]$ (i = 4, 5)

Compound	Mesophase sequence[a]	Transition temperature T/°C	ΔH/kJ mol^{-1}		ΔS/J mol^{-1} K^{-1}	
			tot[d]	*meso*[e]	tot[d]	*meso*[e]
L4[b]	g→N	38	—	—	—	—
	N→I	200	4.4	2.2	9.3	4.7
L5[b]	g→N	35	—	—	—	—
	N→I	132	5.9	3.0	14.6	7.3
$[Mn_{12}O_{12}(\mathbf{L4}\text{-H})_{16}(H_2O)_4]$[c]	g→SmA	40	—	—	—	—
	SmA→I	202	75.4	2.4	158.7	5.0
$[Mn_{12}O_{12}(\mathbf{L5}\text{-H})_{16}(H_2O)_4]$[c]	g→SmA	40	—	—	—	—
	SmA→I	138	120.0	3.8	292.0	9.1

[a] g = glassy state, N = nematic phase, SmA = Smectic A phase, I = isotropic fluid. [b] The liquid crystalline phases were identified from their optical textures by POM. [c] The liquid crystalline phases were identified from SA-XRD studies. [d] ΔH_{tot} and ΔS_{tot} are the total enthalpy and entropy changes. [e] $\Delta H_{meso} = \Delta H_{tot}/n_{meso}$ and $\Delta S_{meso} = \Delta S_{tot}/n_{meso}$ are the enthalpy and entropy changes per mesogenic cyanobiphenyl unit (n_{meso} = 2 for **L*i*** and n_{meso} = 32 for $[Mn_{12}O_{12}(\mathbf{L}i\text{-H})_{16}(H_2O)_4]$). Temperatures are given for the onset of the peaks observed during the second heating processes.

occurrence of liquid-crystalline mesophases (Table 1). The thermal behaviours of the clusters $[Mn_{12}O_{12}(\mathbf{L}i\text{-H})_{16}(H_2O)_4]$ closely mirror those of their mesogenic precursors **L*i*** (i = 4, 5; Fig. 1 and Fig S9–10, ESI†), as previously reported for the related systems **L*i*** (i = 2, 3) and their corresponding complexes $[Ln\mathbf{L}i(NO_3)_3]$ (i = 2, 3).[15c] The calculation of comparable thermodynamic enthalpy and entropy changes occurring at the clearing temperature per cyanobiphenyl unit for the free and complexed dendrimeric ligands ($\Delta H_{meso.}$ and ΔS_{meso} in Table 1) indeed confirm the minor role played by the metallic clusters on the clearing processes, overwhelmed by the organic moieties.

Small-angle X-ray Diffraction (SA-XRD) pattern recorded in the 40–200 °C range showed two sharp reflections in the low-angle region, which were indexed with the 001, 002 Miller indices of a 1D lamellar ordering with a lattice parameter $d = \frac{1}{2}(d_{001(exp)} + 2d_{002exp)}) \approx 87$ Å (Fig. 2a, Table 2, Fig. S8 and Table S2, ESI†). The interlayer distances are only weakly temperature-dependent and, beyond the standard broad diffraction peak centred at 4.5 Å which can be assigned to molten alkyl chains, an additional broad reflection (d') centred around 23 Å was displayed by both clusters. This pattern has been tentatively assigned to the average in-plane intercluster distance, *i.e.* an intralayer order associated with a specific arrangement of the strongly diffracting polymetallic magnetic core. The low-intensity and relative broadness of this reflection suggests nevertheless that this order does not propagate to long distances and is rather loose.

Except for the expected sizable decrease of the clearing temperature (ΔT_c = 64 degrees) observed upon methylation of the terminal cyanobiphenyl mesogens ($[Mn_{12}O_{12}(\mathbf{L5}\text{-H})_{16}(H_2O)_4]$ *versus* ($[Mn_{12}O_{12}(\mathbf{L4}\text{-H})_{16}(H_2O)_4]$) (Fig. 2 and Table S2†), the liquid crystalline supramolecular organization in smectic-like phases of both clusters is very similar. The periodicities recorded for the lamellar phases suggest that the dendronized clusters most probably adopt an extended cylindrical conformation, in which the peripheral mesogenic end-groups are equally distributed on either side of the metallic cluster as in liquid-crystalline end-caped dendrimers.[18] This arrangement is obviously governed by the strongly interacting cyanobiphenyl end-groups, since in such a conformation the Mn_{12} cores, located at the focal point of sixteen $[\mathbf{L}i\text{-H}]^-$ (i = 4, 5) ligands and thus being therefore too distant from the interfaces by approximately 40 Å, are not able to sterically interact. From estimated molecular volumes, considering a density of *ca.* 1 g cm^{-3} for both clustomesogens ($V_{mol} \approx 410\,730$ and 42 470 Å^3 for $[Mn_{12}O_{12}(\mathbf{L4}\text{-H})_{16}(H_2O)_4]$ and ($[Mn_{12}O_{12}(\mathbf{L5}\text{-H})_{16}(H_2O)_4]$, respectively), the calculated molecular areas $A_{mol} = V_{mol}/d = 476.9$ and 489.3 Å^2, respectively, and the associated mesogenic cross-section areas $a_{mes} = A_{mol}/16 = 29.8$ and 30.6 Å^2, respectively, confirm the cylindrical conformation adopted by the clustomesogens in the smectic phase (standard value a_{mes} = 22 Å^2), with slight tilt and/or partial interdigitation between vicinal end-mesogens. The surface area of the short-range time-averaged lattices formed by the cluster core is given by the molecular area. Ideally, two lattice symmetries are therefore possible, either square-like, as previously hypothesized,[13] or hexagonal-like. In the first case, the intercluster distance would be given by $d' = 1.1222\sqrt{A_{mol}}$ and the results give d'-values of 24.5 Å (d'_{max} = 21.8 Å and $2d'_{min}$ = 30.9 Å) and 24.8 Å (d'_{max} = 22.1 Å and $2d'_{min}$ = 31.25 Å), respectively.[19,20] In the hexagonal case, $d' = 0.9763\sqrt{A_{mol}}$ gives mean distances of 21.3 (with d'_{min} = 20.3 Å, d'_{max} = 23.2 Å)[19] and 21.6 Å (with d'_{min} = 20.5 Å, d'_{max} = 23.8 Å), respectively.[19,20] The calculated distances considering the hexagonal symmetry are in good agreement with the measured ones, in contrast to those obtained for a square-like lattice, substantially diverging. Although, considering the broadness of the corresponding reflections, it seems *a priori* daring to discriminate between one or the other lattice type. Such a fixed in-plane hexagonal order, consisting in exactly six closed neighbours, is however short-range due to the fluid nature of the mesophase, and consequently this average number may slightly diverge from this ideal value.

Table 2 Experimental and modelled lattice parameters d and d' for $[Mn_{12}O_{12}(\mathbf{L}i\text{-H})_{16}(H_2O)_4]$ (i = 4, 5) in the SmA mesophases

Compound	d/Å[a]	d'/Å	d_{MD}/Å[b] Hexagonal[b]	d'_{MD}/Å Hexagonal[b]
$[Mn_{12}O_{12}(\mathbf{L4}\text{-H})_{16}(H_2O)_4]$	87.5	22.7	86.7	23.0
$[Mn_{12}O_{12}(\mathbf{L5}\text{-H})_{16}(H_2O)_4]$	86.8	23.3	86.7	22.7

[a] Experimental values. [b] Values obtained from molecular dynamics (MD) modelling.

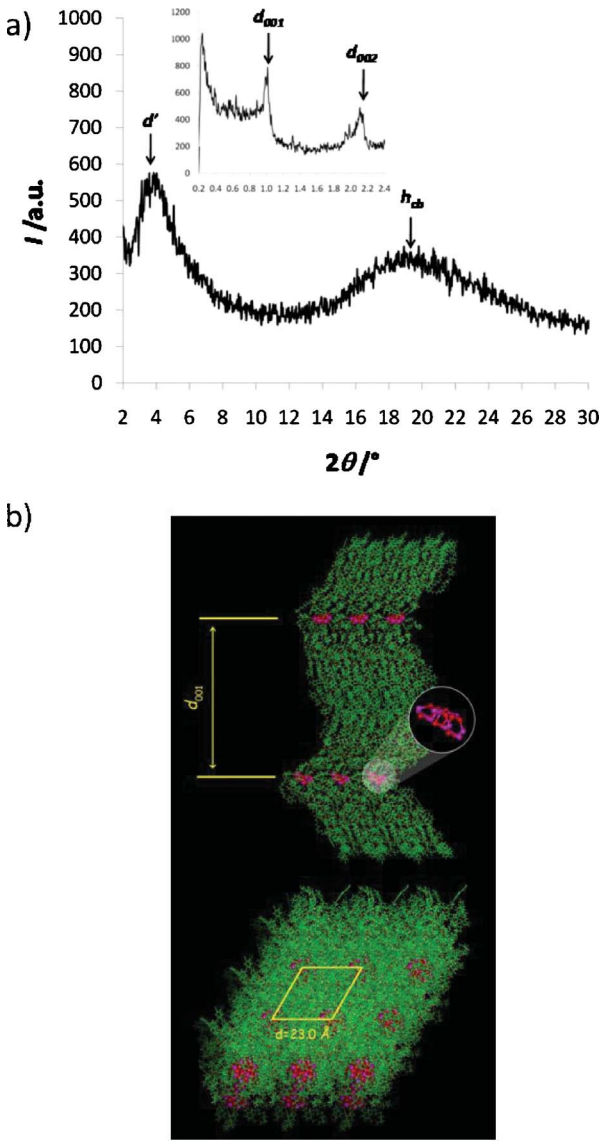

Fig. 2 (a) SA-XRD profile of $[Mn_{12}O_{12}(\mathbf{L5}\text{-H})_{16}(H_2O)_4]$ at 130 °C. (b) View of the computed lamellar packing of $[Mn_{12}O_{12}(\mathbf{L5}\text{-H})_{16}(H_2O)_4]$ in the liquid crystalline phase, parallel (top) and perpendicular (down) to the smectic layers.

In order to validate the liquid crystalline organizations of the two clusters, Molecular Dynamic (MD) simulations were carried out. During the simulation, all the atoms were allowed to move freely except the Mn(III) and Mn(IV) ions for which no suitable field forces were found in any data base. Consequently, the relative positions of the manganese atoms of the central metallic core were restricted according to a static structure.[13] The starting point of the modelling consisted of building a bilayer composed of two clusters with a starting distance higher than the experimental smectic periodicities for avoiding artificially constrained models. The two models for $[Mn_{12}O_{12}(\mathbf{L}i\text{-H})_{16}(H_2O)_4]$ (i = 4, 5) converged to the same lamellar periodicities of d = 86.7 Å with additional d' = 23.0 (i = 4) and 22.7 Å (i = 5) for (imposed) hexagonal periodicities within the layers, specific values in good agreement with the experimental results (Table 2). This contrasts with the previous MD modelling experiments performed on $[Mn_{12}O_{12}(\mathbf{L1}\text{-H})_{16}(H_2O)_4]$,[13] which evidenced a local square-like organization of the metallic clusters. The significant difference found in the supramolecular organization within the SmA mesophases in $[Mn_{12}O_{12}(\mathbf{L1}\text{-H})_{16}(H_2O)_4]$ and $[Mn_{12}O_{12}(\mathbf{L}i\text{-H})_{16}(H_2O)_4]$ (i = 4, 5) is a direct consequence of the ligand structures. Since $[\mathbf{L1}\text{-H}]^-$ is shorter and more rigid than $[\mathbf{L}i\text{-H}]^-$ (i = 4, 5), the cyanobiphenyl mesogens are located closer to the Mn_{12} core in $[Mn_{12}O_{12}(\mathbf{L1}\text{-H})_{16}(H_2O)_4]$ and the symmetry of the cluster (S_4) propagates through the ligand structure, which eventually constrains the symmetry of the intermolecular packing.

In conclusion, we have established that the single methylation of the peripheral mesogenic cyanobiphenyl groups sufficiently affects the intermolecular cohesion to decrease the melting temperature by more than 60 °C in going from **L4** to **L5** (or from $[Mn_{12}O_{12}(\mathbf{L4}\text{-H})_{16}(H_2O)_4]$ to $[Mn_{12}O_{12}(\mathbf{L5}\text{-H})_{16}(H_2O)_4]$). According to the relatively small volume occupied by the central metallic Mn_{12} cluster in $[Mn_{12}O_{12}(\mathbf{L}i\text{-H})_{16}(H_2O)_4]$ (i = 4, 5) and the strong influence of the remote cyanobiphenyl groups on the intermolecular cohesion, we expected and indeed observed that the melting temperatures in the free ligand and in its complexes were very similar. Given that the introduction of bulky metallic cores in liquid crystalline phases still remains a considerable challenge,[2,3,21] the use of specifically-substituted peripheral mesogenic groups decorrelated from the active metallic clusters may offer attractive perspectives for designing functional metallomesogens.

Acknowledgements

Financial support from the Swiss National Science Foundation is gratefully acknowledged.

Notes and references

1 S. A. Claridge, A. W. Castleman, Jr., S. N. Khanna, C. B. Murray, A. Sen and Paul S. Weiss, *ACS Nano*, 2009, **3**, 244.
2 (*a*) W. Li, S. Yi, Y. Wu and L. Wu, *J. Phys. Chem. B*, 2006, **110**, 16961; (*b*) W. Li, S. Yin, J. Wang and L. Wu, *Chem. Mater.*, 2008, **20**, 514; (*c*) S. Yin, W. Li, J. Wang and L. Wu, *J. Phys. Chem. B*, 2008, **112**, 3983; (*d*) S. Yin, H. Sun, Y. Yan, W. Li and L. Wu, *J. Phys. Chem. B*, 2009, **113**, 2355; (*e*) Y. Yang, Y. Wang, H. Li, W. Li and L. Wu, *Chem.–Eur. J.*, 2010, **16**, 8062; (*f*) X. Lin, W. Li, J. Zhang, H. Sun, Y. Yan and L. Wu, *Langmuir*, 2010, **26**, 13201.
3 Y. Molard, F. Dorson, V. Circu, T. Roisnel, F. Artzner and S. Cordier, *Angew. Chem., Int. Ed.*, 2010, **49**, 3351.
4 T Hegmann, H. Qi and V. M. Marx, *J. Inorg. Organomet. Polym. Mater.*, 2007, **17**, 483.
5 K. Binnemans, *Chem. Rev.*, 2009, **109**, 4283.
6 C. Walter, *Scientific American*, August 2005.
7 D. Gatteschi and R. Sessoli, *Angew. Chem., Int. Ed.*, 2003, **42**, 268 , and references therein.
8 G. Rogez, B. Donnio, E. Terazzi, J.-L. Gallani, J. P. Kappler, J. P. Bucher and M. Drillon, *Adv. Mater.*, 2009, **21**, 4323.
9 E. Terazzi, S. Suarez, S. Torelli, O. Mamula, H. Nozary, D. Imbert, J.-P. Rivera, E. Guillet, J.-M. Bénech, G. Bernardinelli, R. Scopelliti, C. Bourgogne, B. Donnio, D. Guillon, J.-C. G. Bünzli and C. Piguet, *Adv. Funct. Mater.*, 2006, **16**, 157.
10 I. M. Saez and J. W. Goodby, *Liq. Cryst.*, 1999, **26**, 1101.
11 T. Chuard, R. Deschenaux, A. Hirsch and H. Schönberger, *Chem. Commun.*, 1999, 2103.
12 T. Lis, *Acta Crystallogr., Sect. B: Struct. Crystallogr. Cryst. Chem.*, 1980, **B36**, 2042.
13 E. Terazzi, C. Bourgogne, R. Welter, J.-L. Gallani, D. Guillon, G. Rogez and B. Donnio, *Angew. Chem., Int. Ed.*, 2008, **47**, 490.
14 N. Grumbach, A. Barla, L. Joly, B. Donnio, G. Rogez, E. Terazzi, J.-P. Kappler and J.-L. Gallani, *Eur. Phys. J. B*, 2010, **73**, 103.

15 (*a*) E. Terazzi, B. Bocquet, S. Campidelli, B. Donnio, D. Guillon, R. Deschenaux and C. Piguet, *Chem. Commun.*, 2006, 2922; (*b*) T. B. Jensen, E. Terazzi, B. Donnio, D. Guillon and C. Piguet, *Chem. Commun.*, 2008, 181; (*c*) T. B. Jensen, E. Terazzi, K.-L. Buchwalder, L. Guénée, H. Nozary, K. Schenk, B. Heinrich, B. Donnio, D. Guillon and C. Piguet, *Inorg. Chem.*, 2010, 8601.

16 (*a*) M. A. Novak, R. Sessoli, A. Caneschi and D. Gatteschi, *J. Magn. Mater.*, 1995, **146**, 211; (*b*) R. Sessoli, D. Gatteschi, A. Caneschi and M. A. Novak, *Nature*, 1993, **365**, 141; (*c*) R. Sessoli, *Mol. Cryst. Liq. Cryst.*, 1995, **274**, 145; (*d*) A. Caneschi, D. Gatteschi and R. Sessoli, *J. Am. Chem. Soc.*, 1991, **113**, 5873.

17 (*a*) R. Sessoli, H.-L. Tsai, A. R. Schake, S. Wang, J. B. Vincent, K. Folting, D. Gatteschi, G. Christou and D. N. Hendrickson, *J. Am. Chem. Soc.*, 1993, **115**, 1804; (*b*) S. M. J. Aubin, Z. Sun, H. J. Eppley, E. M. Rumberger, I. A. Guzei, K. Folting, P. K. Gantzel, A. L. Rheingold, G. Christou and D. N. Hendrickson, *Inorg. Chem.*, 2001, **40**, 2127; (*c*) K. Takeda, K. Awaga and T. Inabe, *Phys. Rev. B: Condens. Matter*, 1998, **57**, R11062; (*d*) J. An, Z.-D. Chen, J. Bian, J.-T. Chen, S.-X. Wang, S. Gao and G.-X. Xu, *Inorg. Chim. Acta*, 2000, **299**, 28.

18 B. Donnio, S. Buathong, I. Bury and D. Guillon, *Chem. Soc. Rev.*, 2007, **36**, 1495.

19 Hexagonal symmetry: $d' = 0.9763\sqrt{S}$, $d'_{max}/d'_{min} = 2/\sqrt{3}$ and $S = d'_{min} \cdot d'_{max}$. Square symmetry: $d'_{max}/d'_{min} = \sqrt{2}$, $S = (d'_{max})^2 = \sqrt{2} \times (d'_{min})^2$, $d'/d'_{max} = 1/\cos\theta$, $\theta \subset 0 - \pi/4 \rightarrow d' = [\sqrt{S} \times \sqrt{4}\log(1+2)]/\pi = 1.1222\sqrt{S}$.

20 M. Marcos, R. Giménez, J.-L. Serrano, B. Donnio, B. Heinrich and D. Guillon, *Chem.–Eur. J.*, 2001, **7**, 1006.

21 A. Santoro, A. M. Prokhorov, V. N. Kozhevnikov, A. C. Whitwood, B. Donnio, J. A. G. Williams and D. W. Bruce, *J. Am. Chem. Soc.*, 2011, **133**, 5248.

